https://rbgeomorfologia.org.br/
ISSN 2236-5664

Revista Brasileira de Geomorfologia

v. 25, nº 2 (2024)

http://dx.doi.org/10.20502/rbg.v24i2.2540

Research article

Pseudo Sliding Plane in Super-Thick Soil Materials Deposit at Ngasinan Deep Landslide Area

Plano pseudodeslizante em depósito de solo superespesso na região profunda do deslizamento de terra em Ngasinan

Anastasia Neni Candra Purnamasari [1,2], Junun Sartohadi [3,4], Eddy Hartantyo [5]

[1] Universitas Gadjah Mada, Graduate School - Department of Environmental Sciences, Yogyakarta, Indonesia. E-mail: anastasia.neni.c@mail.ugm.ac.id.
ORCID: https://orcid.org/0009-0001-6191-6528

[2] Universitas Proklamasi 45 Yogyakarta, Faculty of Engineering, Yogyakarta, Indonesia. E-mail: anastasia.neni@gmail.com
ORCID: https://orcid.org/0009-0001-6191-6528

[3] Universitas Gadjah Mada, Faculty of Agriculture - Department of Soil, Yogyakarta, Indonesia. E-mail: junun@ugm.ac.id.
ORCID: https://orcid.org/0000-0002-0059-8335

[4] Universitas Gadjah Mada, Research Center for Land Resources Management, Yogyakarta, Indonesia. E-mail: junun@ugm.ac.id.
ORCID: https://orcid.org/0000-0002-0059-8335

[5] Universitas Gadjah Mada, Faculty of Natural Sciences - Department of Geophysics, Yogyakarta, Indonesia. E-mail: ehartantyo@ugm.ac.id.
ORCID: https://orcid.org/0000-0003-0257-8730

Received: 25/01/2024; Accepted: 16/05/2024; Published: 05/07/2024

Abstract: The research focuses on analyzing landslides within an area abundant in varying sizes of these occurrences. The research is being conducted in Ngasinan, Bogowonto watershed area in Indonesia. These landslides happened in the consistently loose, deep volcanic sediment, referred to as soil material, over 10 meters thick. The goal of this research is to assess potential sliding plane triggering these landslides within this soil material. To achieve this, a blend of geophysical and soil science methodologies is applied. Geophysical measures, specifically resistivity parameters, discern distinctions within the layers of soil material, determined through geoelectric methods. Additionally, soil science factors like Cation Exchange Capacity (CEC) and dispersing ease are used to evaluate the layers with pseudo-sliding plane. Findings demonstrate varied resistivity values, CEC, and water content across the different material layers. The N1 layer, situated at a 5-meter depth, exhibiting characteristics of 5Y 8/1 color (white), shows a resistivity of 8.7 Ωm, a CEC of 54 meq/100g, and high dispersible. Identified as a potential cause of initial landslides or sliding planes, the N1 layer's distinctive values in resistivity, CEC, and water content validate it as an area of concern for potential landslides. These findings confirm that differences in these factors can serve as an early identification for potential landslide-prone areas.

Keywords: sliding plane; thick soil; landslide

Resumo: A pesquisa se concentra na análise de deslizamentos de terra em uma área com abundância de ocorrências de tamanhos variados desses eventos. Esses deslizamentos ocorrem em sedimentos vulcânicos profundos e consistentemente soltos, conhecidos como material do solo, com mais de 10 metros de espessura. O objetivo é avaliar o potencial de planos de

deslizamento que desencadeiam esses eventos dentro desse material do solo. Para alcançar esse objetivo, é adotada uma combinação de metodologias geofísicas e de ciências do solo. Medidas geofísicas, especialmente os parâmetros de resistividade, discernem distinções dentro das camadas do material do solo, identificadas por métodos geoelétricos. Além disso, fatores científicos do solo, como capacidade de troca catiônica (CEC) e facilidade de assoreamento, são utilizados para avaliar as camadas com potencial de planos pseudodeslizantes. Os resultados demonstram valores variados de resistividade, CEC e teor de água nas diferentes camadas do material. A camada N1, situada a 5 metros de profundidade e exibindo características de cor 5Y 8/1 (branco), apresenta resistividade de 8,7 Ωm, CEC de 54 meq/100g e alta suscetibilidade ao assoreamento. Identificada como uma possível causa de deslizamentos de terra iniciais ou planos de deslizamento, os valores distintivos da camada N1 em resistividade, CEC e conteúdo de água a validam como uma área de preocupação para potenciais deslizamentos de terra. Essas descobertas confirmam que as diferenças nesses fatores podem servir como uma identificação precoce de áreas potencialmente propensas a deslizamentos de terra.

Palavras-chave: plano deslizante; solo espesso; deslizamento de terra

1. Introduction

The upper region of Purworejo Regency (Indonesia) is prone to landslides, given its mountainous terrain situated between the Sumbing Volcano and the Nanggulan structural mountains. This area, recognized as a transition zone between volcanic and structural zones, results in the accumulation of thick soil composed of volcanic and weathered rock materials. The research focus lies in the upper Purworejo area within the Bogowonto watershed, a region marked by numerous landslides. Specifically, the prevalent landslide type in this area is characterized as rotational, where the fault surface exhibits an upward curvature (spoon-shaped), and the landslide movement revolves on an axis parallel to the slope contour (HIGHLAND; BOBROWSKY, 2008).

This study grapples with issues occurring in areas characterized by substantial landslides within exceptionally dense soil. Analysis of aerial photography data and on-site survey information reveals that 42% of the entire research location comprises soil prone to sliding and is currently inactive, yet the extent is likely to expand without effective management interventions. The combined area of soil slide and dormant sections amounts to 181.56 hectares, within the broader research site encompassing 435 hectares. The heightened soil thickness in this region is attributable to its transitional positioning, situated between the quarter zone and the tertiary zone (PULUNGAN; SARTOHADI, 2018). The interplay between the quarter and tertiary zones contributes to the formation of dense soil with potential variations in soil properties. Although thick soil exhibits a relatively consistent texture, it is comprised of distinct layers (NOVIYANTO et al., 2020; PULUNGAN; SARTOHADI, 2018; SARTOHADI et al., 2018; WIDA et al., 2019).

In the research area, landslides within the dense soil predominantly manifest as soil slides. The observed landslide types encompass rotational slides, creep, and dormant occurrences. Clay/silt rotational slide ("soil slump") is sliding of a mass of (homogeneous and usually cohesive) soil on a rotational rupture surface (HUNGR et al., 2014). Creep is imperceptibly slow, steady, downward and outward movement of slope forming material (SINGH; PRADHAN; VISHAL, 2019). At the research site, landslides are induced by subsurface creep, specifically observed as subsurface movement causing gradual deformation. This creeping phenomenon is widespread, occurring in various locations, including dormant areas. Dormant is an inactive landslide that can be reactivated (LEE; JONES, 2004). In the research vicinity, dormant areas have been repurposed by local residents as integrated gardens. A significant portion of the landslide-affected terrain at the base has been converted into agricultural land, and some residents have established their homes in these dormant zones. The focal point of further study lies in landslides and their associated scars extensively utilized by the community. A critical aspect involves an initial

assessment to determine the presence of a landslide sliding plane, with emphasis on estimating the sliding plane by analyzing variations in layers within the exceptionally thick soil.

In the context of this study, the term "landslide sliding plane" pertains to the visible and identifiable region where the landslide movement has occurred. Typically, the extensively discussed landslide sliding plane is situated at the contact zone between durable rock formations and sedimentary soil materials (PRATIWI; SARTOHADI; WAHYUDI, 2019). However, the mentioned pseudo sliding plane in this context is a plane that can manifest within variations in the layering of the sedimentary material itself. Understanding the traits of exceptionally thick sediment or soil material is crucial for the preliminary identification of discrepancies in layering. Material layers means to lithology of thick material sediment. Lithology is considered to be one of the main decisive factors in landslide susceptibility assessment that is different of soil layer (DE BRITO, 2017). To achieve subsurface characterization, geophysical data or information on physico-chemical soil properties can be employed.

Information regarding geophysical measurements of sedimentary soil materials is seldom widely disseminated. This is primarily attributed to the challenging and expensive nature of collecting field geophysical data. In contrast, data concerning the physical and chemical properties of soil for agricultural purposes are more readily available. To bridge this gap, this study opts for straightforward geophysical techniques to discern variations in material layers. The geoelectric method is employed to assess resistivity values for each layer of material deposits, providing a means to correlate surface soil data used in agriculture with geophysical insights. The geoelectric method stands out as a valuable tool for subsurface mapping in this study (CRAWFORD et al., 2018). The geoelectric method is a geophysical technique grounded in the fundamental principles of Ohm's law (AN et al., 2020). The outcomes derived from this method yield resistivity values as a measure of subsurface electrical resistance (AHN et al., 2022; BRUNET et al., 2010; GIAMBASTIANI et al., 2022).

The assessment of physical and chemical characteristics of soil has been extensively conducted in agricultural areas with the aim of enhancing plant productivity (BENSA, 2022). Soil survey activities for agriculture routinely involve measuring physico-chemical properties such as water content, specific gravity, bulk volume, texture, and cation exchange capacity. The landslide phenomenon has brought about the elevation or exposure of soil layers that were originally situated deeper than 2 meters, consequently making them subjects of agricultural land surveys (NOVIANTO et al., 2020). There exists the potential for a correlation between the physical and chemical attributes of the soil and the geophysical properties of the material, particularly resistivity, commonly utilized for identifying sliding plane.

The recognition of landslide sliding plane serves as a foundational step for subsequent extensive surveys or research involving large-scale geophysical measurements. These measurements prove valuable in regions lacking surface outcrops, enabling thorough subsurface mapping. Subsurface maps, in turn, contribute to a clear understanding of the presence of landslide sliding plane. The data acquired from this research will be utilized as crucial input for implementing landslide mitigation strategies, particularly benefiting the communities residing in the vicinity of Ngasinan.

2. Study area

The research is located in Purworejo, Central Java, Indonesia, specifically within the Bogowonto watershed. The survey and soil sampling activities are conducted across this watershed, as indicated by the red dots in Fig.1. The central Bogowonto watershed is in the transition zone between the quarter zone and the tertiary zone (PULUNGAN; SARTOHADI, 2017). The central Bogowonto watershed exhibits a topography marked by slopes

ranging from gentle to very steep (PULUNGAN; SARTOHADI, 2017, 2018). Notably, the delineation of Ngasinan village in Purworejo, Central Java, Indonesia, is represented by the black line in the study area (Fig.1).

The transition zone is characterized by numerous landslides occurring within exceptionally thick sediment and soil material. The research site itself has experienced landslides within such dense sediment and soil. An on-site survey of the research location revealed the prevalence of various phenomena, including creeps, gully erosion, dormant, and landslides. The identification of creep is evident through the observable slope of trees within the mixed garden. Creeping processes are observed both within dormant areas and in the vicinity of settlements within the study area.

Environmental conditions in Ngasinan will be shaped by global factors such as rainfall patterns, the characteristics of the rainy and dry seasons, as well as local temperature and vegetation. The rainy season in Ngasinan, aligned with Indonesia's rainy season, spans from September to February, while the dry season extends from March to August. However, these seasons are influenced by broader global climate patterns. Situated on the slopes of the Sumbing Volcano, Ngasinan has cooler temperatures compared to lower-lying areas. The region's diverse land cover includes rice fields, mixed gardens, and various organizations. The rice fields support different crops depending on the planting season, while the mixed gardens feature a variety of plants and trees such as bamboo, coconut, duku tree (*Lansium domesticum*), and durian tree (*Durio zibethinus Murr.*).

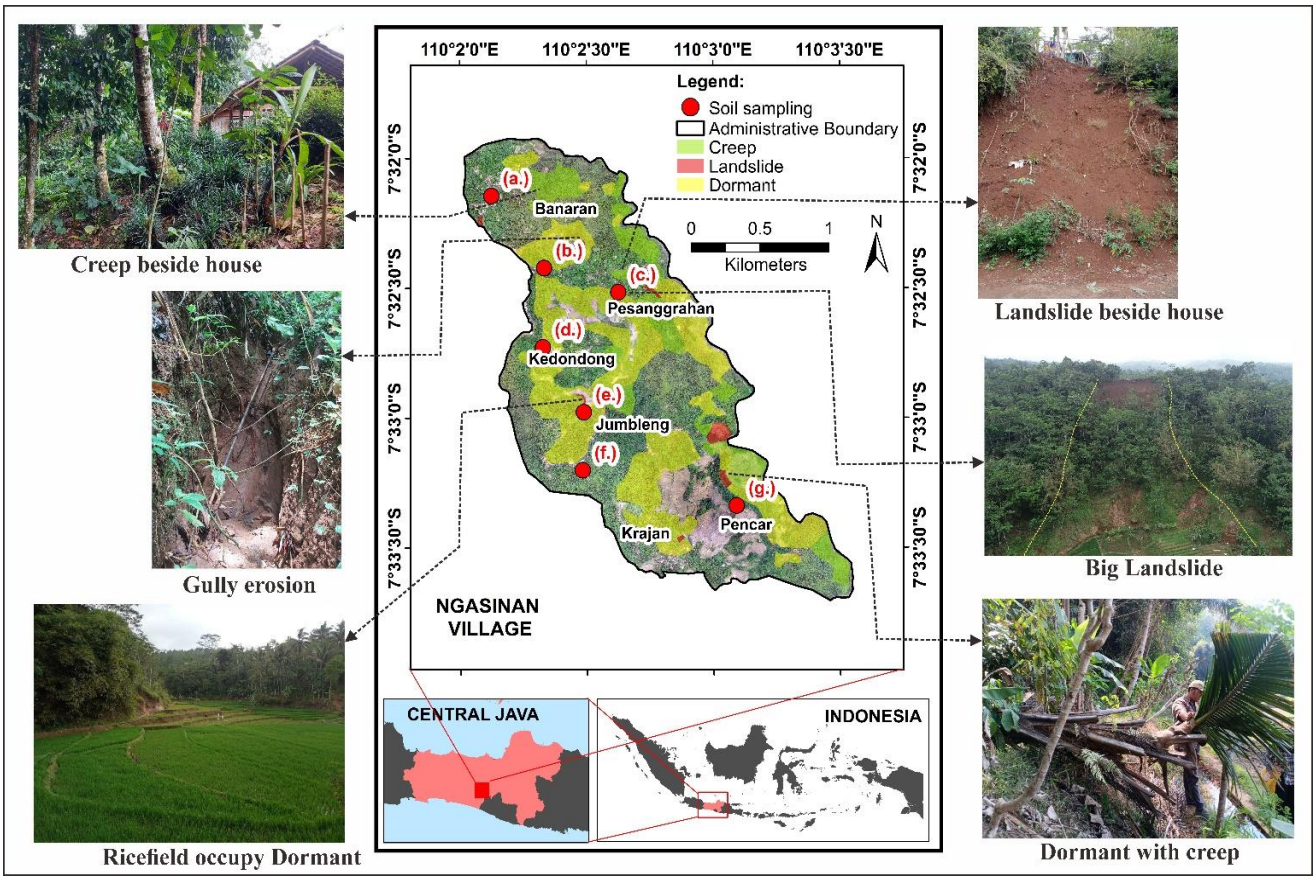

Fig. 1. Study area.

3. Materials and Methods

3.1. Fields survey and soil sampling

The employed methodology in this research involves a direct field survey, commencing with the identification of soil material layers, as illustrated in Fig.1. The field survey is specifically conducted at landslide sites to pinpoint soil layers suspected to possess a high potential as pseudo-sliding plane. Samples are systematically collected from each soil layer for subsequent resistivity measurements in the laboratory. Through these resistivity measurements, distinctions in resistivity values for each layer of material deposits are determined. The variation in resistivity values serves as a valuable reference for assessing the potential for pseudo-sliding plane within the exceptionally thick soil.

The field survey was expanded in the vicinity of the landslide point with the objective of identifying soil layers with the potential to transform into sliding plane. The initial step involved distinguishing layers based on soil color. Subsequent surveys around the landslide location were conducted to examine additional soil layers close to the surface. This evaluation aimed to assess the potential for pseudo-sliding plane, utilizing resistivity values as a key criterion.

Soil sampling and measurements were conducted during the transitional period between the rainy season and the dry season, ensuring optimal soil conditions that are neither excessively wet nor overly dry. Three distinct types of soil samples were collected from each layer, specifically sourced from outcrops of the super thick soil. The layers sampled and measured from the outcrop are visually represented in Fig. 2, while the soil sampling process is illustrated in Fig. 3. The first sample is designated for measuring the resistivity of the undisturbed soil, the second sample is a disturbed sample utilized for determining CEC (cation exchange capacity), and the third sample is designated for assessing the water content of the undisturbed soil using a ring.

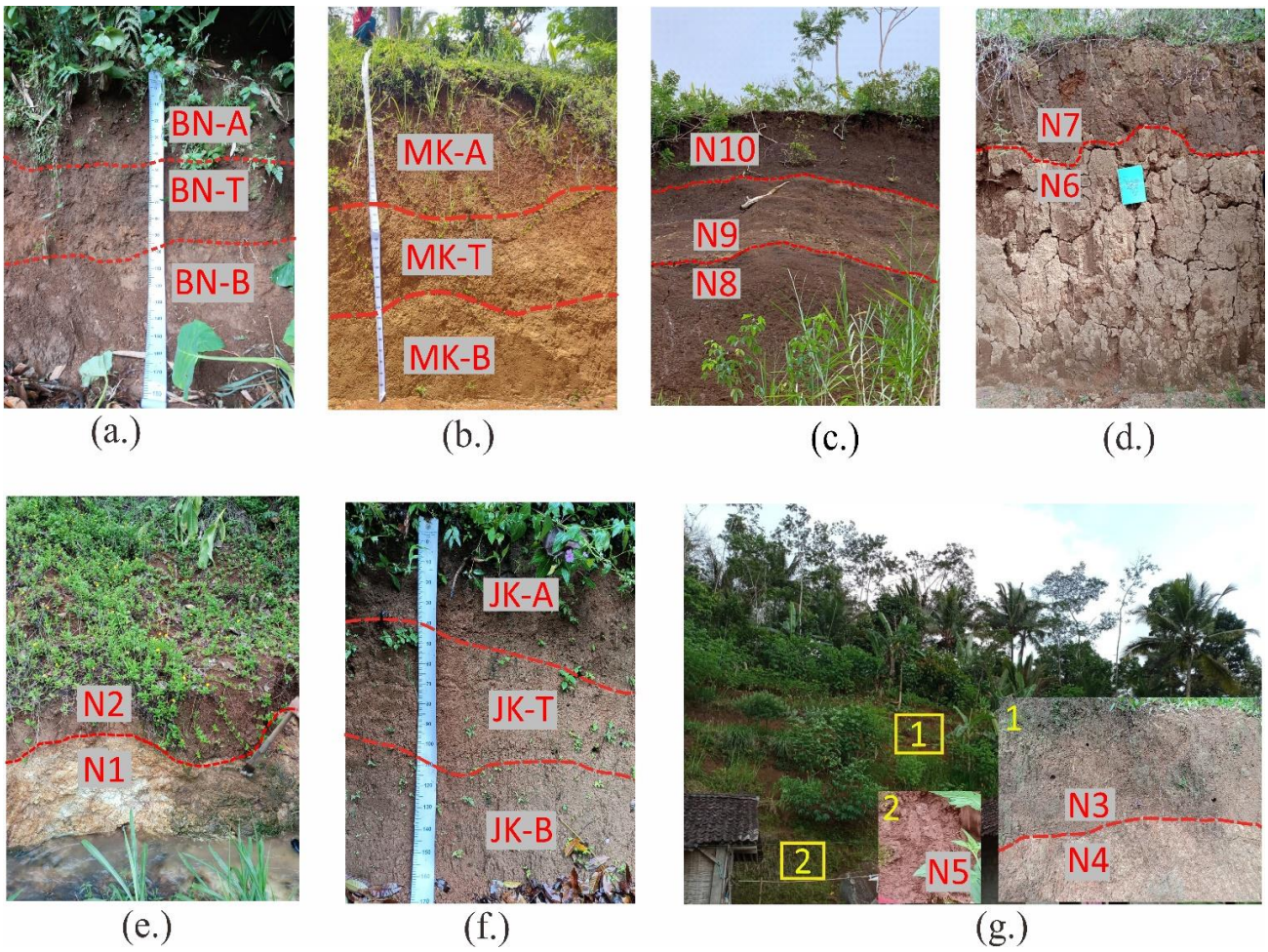

Fig. 2. Field view of the studied; (a.) – (g.) layers material in the outcrop.

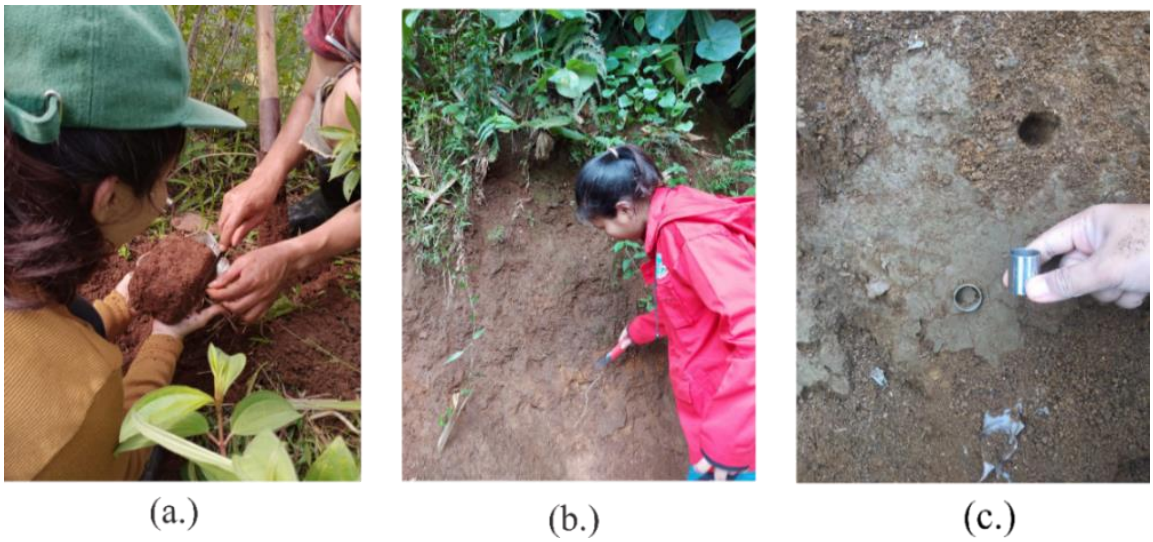

Fig. 3. Soil sampling; (a.)resistivity, (b.)CEC dan (c.)water content.

3.2. Geophysics measurement

Resistivity measurements are conducted employing geophysical techniques, specifically through the application of geoelectricity. The fundamental principle underlying laboratory resistivity measurements aligns with the principles guiding field geoelectric measurements. The chosen configuration for these measurements is the Wenner configuration, as depicted in Fig. 4(a.). The utilization of the Wenner alpha method is based on its sensitivity to vertical changes, making it well-suited for the intended purposes of the study (TELFORD et al., 1990). The emphasis on vertical changes in the geoelectric method stems from the specific objective of measuring resistivity values for each individual soil layer. This method is extensively employed in soil and rock research, offering a valuable means to examine and quantify the resistivity values associated with different layers of soil and rock (MALICK ROSVELT et al., 2022; SÉGER et al., 2009; ZUO et al., 2021). Resistivity measurements in situ on rock samples can be conducted using the identical configuration employed for field measurements (Rekapalli et al., 2014). The principle of the geoelectric method is Ohm's law (HASAN et al., 2021) with the formula (1).

$$R = \frac{V}{I} \tag{1}$$

with R= resistivity (ohm meter)
V= voltage (volt)
I= current (ampere)

C1, C2, P1, and P2 represent electrodes organized in a Wenner configuration, where the inter-electrode distance is denoted as 'a.' Resistivity measurements of laboratory samples were conducted twice. The calculations align with the Wenner configuration formula, specifically incorporating the 'k' value from formulas (2) and (3), resulting in the determination of the apparent resistivity value (ISMAIL et al., 2022).

$$k = 2\pi a \tag{2}$$

$$\rho_s = k \cdot \frac{V}{I} \tag{3}$$

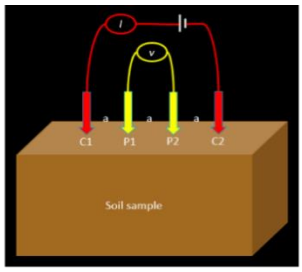

(a.)

(b.)

(c.)

Fig. 4. Geoelectric methods; (a.)wenner configuration, (b.)laboratory measurement, (c.)field measurement

In addition to laboratory resistivity measurements, field resistivity measurements were also undertaken to facilitate a comparative analysis of sample resistivity values. Consistency in configuration was maintained between laboratory and field measurements, with both employing the Wenner configuration. Geoelectric measurements in the field, illustrated in Fig. 4(b.) and Fig. 4(c.), utilized the same Oyo mc Ohm tool equipped with small electrodes. Traditional geophysical survey research, especially in geoelectrics, typically involves extensive equipment and high costs, often incorporating lengthy trajectories and large electrodes (JOSHI et al., 2021; LOWE et al., 2017; MERRITT et al., 2016). Notably, this resistivity research presents a simpler and more cost-effective alternative compared to conventional geoelectric investigations.

3.3. Soil characterization

The outcomes of the survey and resistivity measurements underwent validation through an agricultural survey, aiming to establish a connection between resistivity values and soil characteristics. The acquired results are qualitatively discussed in correlation with data on basic physical and chemical soil properties, commonly derived from agricultural soil surveys. The chemical parameter considered in this context is the cation exchange capacity, while the physical aspect involves the soil water content. This qualitative discussion aims to illuminate the interrelation between resistivity measurements and fundamental soil characteristics.

In the realm of soil science in agriculture, cation exchange capacity is frequently employed to assess soil characteristics, particularly in understanding the soil's capacity to retain water (BAZOOBANDI, 2022). Cation exchange capacity is highly affected by the number of colloids able to absorb cations in soil (JUHADI et al., 2022). Cation exchange capacity quantifies the soil's ability to attract and exchange cations (Ca^{2+}, Mg^{2+}, K^{+}, Na^{+})(ZHAO et al., 2020). Total cation capacity is the cumulative sum of the individual cation exchange capacities ($CEC = \sum_i CECi$), with i= K^{+}, Na^{+}, Ca^{2+}, Mg^{2+}(SINGLA et al., 2020). The cation exchange capacity value fluctuates for each region based on the chemical composition of the soil in that specific area (BAZOOBANDI, 2022).

Disturbed material or soil samples collected from the field are subsequently processed for cation exchange capacity testing. The methodology employed for testing involves the addition of ammonium acetate (ENANG et al., 2022; SINGLA et al., 2020; SONG et al., 2022). The prepared soil samples, after being weighed and treated with ammonium acetate, undergo an overnight incubation period, followed by filtration using Wattman paper. Subsequent to the filtration process, additional chemicals are introduced, and the sequence continues with distillation and titration. Fig.5(a.) depicts the cation exchange capacity measurement conducted in the laboratory.

Among the physical properties scrutinized in soil science and agriculture, soil water content assumes significance (BOURENNANE et al., 2012; BRUNET et al., 2010; CHEN et al., 2019; MIRACAPILLO; MOREL-SEYTOUX, 2015; SUN et al., 2020). It serves as a medium for conductivity, facilitating the flow of electricity (SAMOUËLIAN et al., 2005). There exists a correlation between soil water content and resistivity, wherein higher water content corresponds to a decrease in resistivity values (MELO et al., 2021).

Undisturbed soil, obtained using a ring, undergoes field water content measurement (actual water). The process involves weighing the soil from the field, subjecting it to a 24-hour oven treatment, and subsequently reweighing it. Saturated water content is determined by contrasting the oven-treated soil with soil that has been saturated for 24 hours. The difference in water content is then computed as the saturated water content minus the field water content. This discrepancy in water content serves as a method for assessing the soil's susceptibility to dispersion. The ease of dispersion pertains to how readily the soil becomes saturated with water. Table 1 illustrates the distribution of ease of dispersion levels, categorized into low, medium, and high. Fig. 5(b.) illustrates the water content measurement activity conducted in the laboratory.

Fig. 5. Soil characterization; (a.)CEC laboratory measurement, and (b.)water content laboratory measurement

Tabel 1 . Difference in water content with level of ease of dispersing

Difference in water content (%)	level of ease of dispersing
< 0	low
0 - 20	medium
> 20	high

4. Results

The preliminary identification of thick soil layers is initiated by observing the color of the soil material. The contrast in layer color serves as an initial indicator of potential variations in soil resistivity values. Table 2 illustrates that layers with distinct colors correspond to diverse resistivity values. The resistivity measurements exhibit a range of values. Notably, the N1 layer displays a minimal resistivity value, specifically 8.7 Ωm. A smaller resistivity value implies a higher conductivity value, which can stem from elevated water content or the impact of chemical composition within the deposited material or soil.

The resistivity measurements obtained at survey points, whether conducted in the laboratory or in the field, exhibit a consistent trend. It is imperative to establish correlations between resistivity results and other material/soil characteristics. The material/soil characteristics chosen for correlation include cation exchange capacity and water content. The respective values for resistivity, cation exchange capacity (CEC), and water content are detailed in Table 2.

Cation exchange capacity values exhibit a range of variations, signaling distinct values across different layers. These disparities in cation exchange capacity values imply discrepancies in the chemical composition of the material/soil. Within the realm of agriculture, cation exchange capacity serves as a pivotal soil property for assessing soil fertility. The diversity in CEC chemical content can be a crucial factor to correlate with other material/soil characteristics such as resistivity and water content. Notably, sample N1 stands out with a high CEC value, measuring at 54 meq/100g.

Tabel 2. Soil Characterization

No	Soil layer	Color	Resistivity (Ωm)	CEC (meq/100g)	Field water content (%)	Saturated water content (%)	Difference in water content (%)
1	JK-A	5YR 4/6	29.68	17.04	55.14	49.10	-6.03
2	JK-T	2.5YR 3/6	27.21	16.21	49.71	46.49	-3.21
3	JK-B	5YR 3/4	52.15	14.55	46.32	40.12	-6.20
4	MK-A	5YR 5/8	163.25	22.93	43.26	43.48	0.22
5	MK-T	2.5YR 5/8	91.97	26.97	44.97	48.13	3.16
6	MK-B	7.5YR 5/8	48.01	23.95	43.87	43.28	-0.58
7	BN-A	2.5YR 2.5/4	132.76	20.39	68.73	59.04	-9.69
8	BN-T	5YR 5/8	143.86	10.14	83.33	79.61	-3.72
9	BN-B	10YR 6/4	104.80	12.12	97.62	55.58	-42.04
10	N1	5Y 8/1	8.70	54	57.47	80.87	23.39
11	N2	5YR 4/6	54.03	18.4	57.31	55.77	-1.54
12	N3	7.5YR 4/6	76.83	21	35.62	54.37	18.75
13	N4	5YR 5/8	133.29	13	39.71	50.22	10.51
14	N5	2.5YR 5/6	139.77	14.2	54.82	58.40	3.58
15	N6	7.5R 3/4	316.46	23.2	58.15	49.25	-8.89
16	N7	10YR 3/6	386.17	25.6	57.64	73.29	15.64
17	N8	7.5YR 2.5/3	51.38	22	48.85	69.63	20.79
18	N9	7.5YR 3/4	135.08	13.2	45.56	50.28	4.72
19	N10	7.5YR 3/3	81.81	19	44.20	62.00	17.80

The subsequent soil characteristic measured is water content. Field or actual soil water content pertains to the water content in direct soil samples that have not undergone saturation. In contrast, saturated soil water content refers to the water content of samples subjected to the saturation process by soaking in water. The disparity between field soil water content and saturated soil water content is utilized to categorize the level of ease of dispersing. The classification of the ease of dispersing for each sample layer in the studied material is presented in Fig. 6. Notably, samples N1 and N8 exhibit a high level of dispersing.

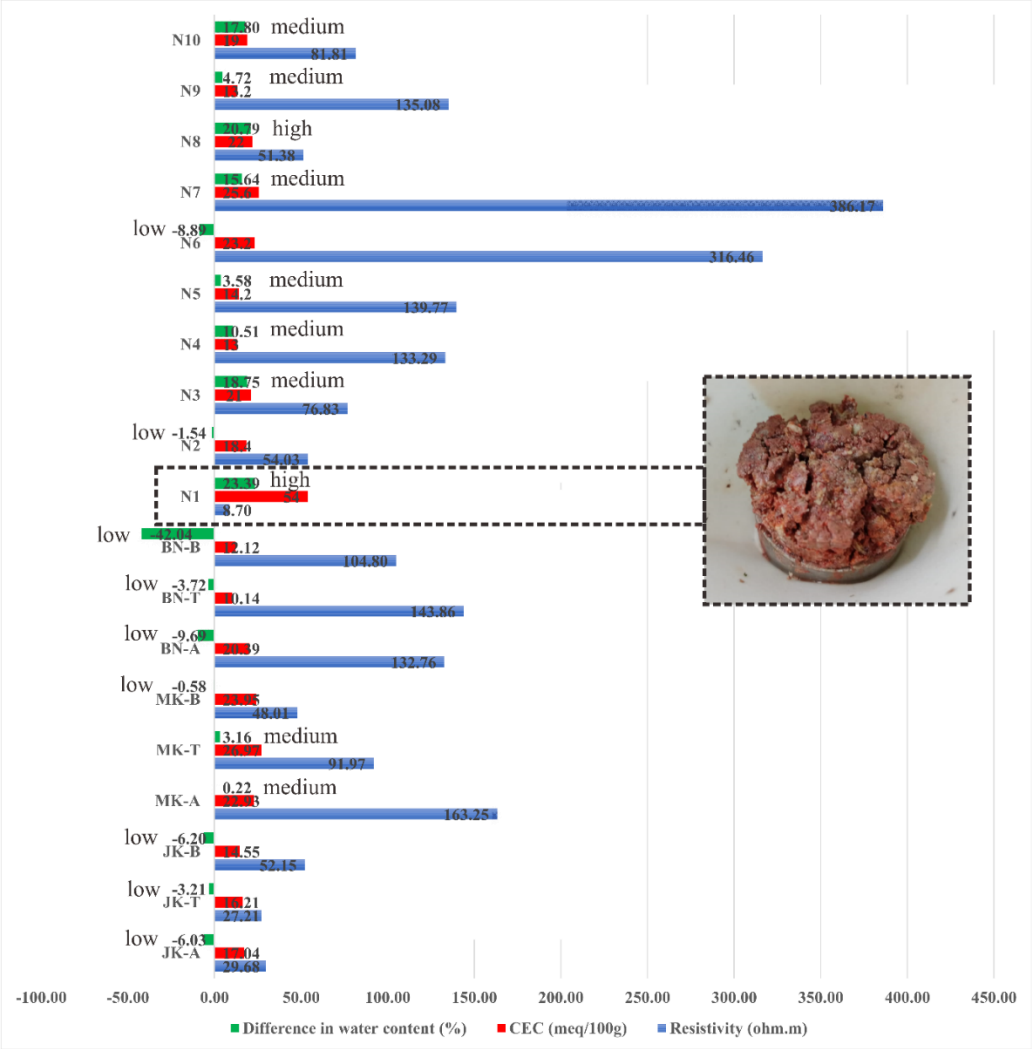

Fig. 6. Result comparison between resistivity, CEC, and difference in water content

In certain soil material samples, the saturated water content is lower than the field water content. This discrepancy arises due to the amorphous nature of minerals resulting from volcanic weathering (FIANTIS et al., 2010, 2011; FIANTIS et al., 2009). Layers characterized by a low susceptibility to siltation necessitate an extended duration to reach full saturation with water. The ease of dispersing is intricately connected to both the physical properties and chemical content of the material layer.

5. Discussion

The interpretation of resistivity, cation exchange capacity (CEC), and water content measurement results involves a comprehensive review of field observations at the research location. The resistivity values are correlated with water content, a parameter influenced by weather conditions and irrigation practices. Material sampling and field resistivity measurements were executed during the transitional season between the rainy and dry periods, an ideal timeframe for geoelectric measurements to ascertain resistivity values for soil material layers. The resistivity value is intricately linked to water content, necessitating data collection adjustments aligned with weather and field conditions during sampling and resistivity measurements. The water content in soil material is associated with soil porosity, a key physical characteristic. Fracture porosity, in turn, influences cation exchange capacity and

indicates the presence of clay minerals (DUTILLEUL et al., 2020). While water content is pivotal, the chemical properties of the soil material also warrant consideration.

In the laboratory, the chemical properties of soil materials are assessed through cation exchange capacity analysis conducted on extracted samples. A correlation is observed between resistivity and cation exchange capacity; elevated cation exchange capacity corresponds to reduced resistivity, and conversely, diminished cation exchange capacity aligns with heightened resistivity (WEISENBERGER et al., 2020). Grain size, soil material, texture, and porosity influence both cation exchange capacity and conductivity values (REVIL et al., 2017). The correlation of data concerning differences in water content, resistivity, and cation exchange capacity is illustrated in Fig. 6. Notably, a distinct tendency is evident in the N1 layer material, displaying elevated water content, low resistivity, and high cation exchange capacity values. This tendency suggests that the N1 layer exhibits characteristics conducive to easy water saturation and a high susceptibility to dispers, indicating its potential as a landslide sliding plane.

The N1 layer holds considerable potential as an instigator of initial landslides or sliding plane. Positioned at a depth of 5 meters, the field characteristics of the N1 layer include a 5Y 8/1 color (tending towards white/light), with a resistivity value of 8.7 Ωm, a cation exchange capacity (CEC) of 54 meq/100g, and a pronounced susceptibility to siltation. As depicted in Fig. 6, a sample from the N1 layer, when saturated with water, exhibits rapid expansion, occurring within a matter of seconds. The highly muddy nature of the N1 layer material poses a significant hazard, particularly in research locations characterized by very thick soil. During periods of heavy rainfall, this N1-like layer can swiftly saturate with water, potentially evolving into a landslide pseudo-sliding plane. The friable and easily saturated characteristics of the N1 layer material are attributed to its volcanic ash origin, a factor to consider given the research location's status as a transition zone influenced by the Sumbing Volcano.

In certain layers of material, there exists a moderate susceptibility to siltation, implying its potential as a sliding plane for landslides. The medium level of ease of dispersing is further substantiated by relatively low resistivity values, signifying a relatively loose composition. Layers consisting of relatively loose material are prone to fluid infiltration, rendering them potential landslide sliding plane in the future.

Landslide sliding plane within exceptionally thick soil are termed landslide pseudo-sliding plane. The designation "pseudo" is applied because these slip surfaces are not situated between solid rock layers or directly above the parent rock. The integrated survey involving geophysics and soil science serves as an initial alternative for identifying landslide sliding plane. This preliminary survey can serve as a reference for subsequent research endeavors, such as broader geophysical measurements and the application of additional methods.

6. Conclusion

Differences in layers in super - thick soil, providing an initial indication of potential for landslide sliding plane. The research outcomes highlight layers of soil material that exhibit the propensity to initiate landslides or serve as sliding plane. Identification of a pseudo-sliding plane is achievable through laboratory measurements on loose volcanic ash deposits. Loose material layers, characterized by low resistivity values, high cation exchange capacity (CEC), and high dispersibility, denote the potential pseudo-sliding plane within super thick soil material. This pseudo-sliding plane is typified by a white color of 5Y 8/1, showcasing easy dispersing characteristics in laboratory tests with a water content difference ranging from 10% to over 20%. Additionally, the area exhibits low-moderate fertility potential, with CEC values ranging from 10 meq/100g to 55 meq/100g, and geophysically presents resistivity values between 8 Ωm and 52 Ωm. These findings serve as a valuable tool for rapid identification,

leveraging resistivity measurements, CEC values, ease of dispersing assessment, soil color observations, or a combination thereof.

Identifying the presence of a pseudo-sliding plane is crucial for understanding landslides in Ngasinan, a location within the transition zone. This concept can also be applied to other transition zones with similarly thick soil material characteristics. Quickly estimating the existence of pseudo-sliding planes can initiate subsurface mapping research. Subsurface mapping, which employs macro geophysical methods, requires ample to gather data over large areas.

Author Contributions: Anastasia Neni Candra Purnamasari: Conceptualization, Methodology, Software, Field work, Writing-Original draft preparation. **Junun Sartohadi:** Conceptual improvement, Data curation and presentation, Field work assessment, Writing-Reviewing. **Eddy Hartantyo:** Conceptualization, Data curation, Validation, Writing-Reviewing

Financing: This research has a funding from BPPT and LPDP, but do not have funding for publication.

Acknowledgment: Authors wish to thank the Center for Higher Education Funding (BPPT) and Indonesia Endowment Funds for Education (LPDP) for the research funding. This paper is part of a research dissertation entitled Environmental Geopedophysics Studies in Landslide Areas Around Ngasinan Village, Purworejo, Central Java.

Conflict of interest: The authors declare that there is no conflict of interest. The funders had no interference in the development of the study; in the data collection, -analysis, or -interpretation; in the writing of the manuscript, or in the decision to publish the results.

References

1. AHN, Y.; HAN, M.; CHOI, J. Effect of electrode types and soil moisture on the application of electrical resistivity tomography and time-domain induced polarization for monitoring soil stabilization. **Measurement: Journal of the International Measurement Confederation**, v. 187, p. 110220, 2022. DOI: 10.1016/j.measurement.2021.110220
2. AN, N.; TANG, C. S.; CHENG, Q.; WANG, D. Y.; SHI, B. Application of electrical resistivity method in the characterization of 2D desiccation cracking process of clayey soil. **Engineering Geology**, p. 265, 2020. DOI: 10.1016/j.enggeo.2019.105416
3. BAZOOBANDI, A. Prediction of Soil Cation Exchange Capacity Using Enhanced Machine Learning Approaches in Southern Region of the Caspian Sea of Iran. **Ain Shams Engineering Journal**, v. xxxx, p. 101876, 2022. DOI: 10.1016/j.asej.2022.101876
4. BENSA, A. Evaluation of Vis-NIR preprocessing combined with PLS regression for estimation soil organic carbon , cation exchange capacity and clay from eastern Croatia. **Geoderma Regional**, v. 30, 2022. DOI: 10.1016/j.geodrs.2022.e00558
5. BESSON, A.; COUSIN, I.; SAMOUËLIAN, A.; BOIZARD, H.; RICHARD, G. Structural heterogeneity of the soil tilled layer as characterized by 2D electrical resistivity surveying. **Soil and Tillage Research**, v. 79, p. 239–249, 2004. DOI: 10.1016/j.still.2004.07.012
6. BOURENNANE, H.; NICOULLAUD, B.; COUTURIER, A.; PASQUIER, C.; MARY, B.; KING, D. Geostatistical filtering for improved soil water content estimation from electrical resistivity data. **Geoderma**, v. 183–184, p. 32–40, 2012. DOI: 10.1016/j.geoderma.2012.03.008
7. BRUNET, P.; CLÉMENT, R.; BOUVIER, C. Monitoring soil water content and deficit using Electrical Resistivity Tomography (ERT) - A case study in the Cevennes area, France. **Journal of Hydrology**, v. 380, n. 1–2, p. 146–153, 2010. DOI: 10.1016/j.jhydrol.2009.10.032
8. CHEN, B.; GARRÉ, S.; LIU, H.; YAN, C.; LIU, E.; GONG, D.; MEI, X. Two-dimensional monitoring of soil water content in fields with plastic mulching using electrical resistivity tomography. **Computers and Electronics in Agriculture**, v. 159, p. 84–91, 2019. DOI: 10.1016/j.compag.2019.02.028
9. CRAWFORD, M. M.; BRYSON, L. S.; WOOLERY, E. W.; WANG, Z. Using 2-D electrical resistivity imaging for joint geophysical and geotechnical characterization of shallow landslides. **Journal of Applied Geophysics**, v. 157, p. 37–46, 2018. DOI: 10.1016/j.jappgeo.2018.06.009

10. DE BRITO, M.; WEBER, E.; DA SILVA FILHO, L. Multi-criteria analysis applied to landslide susceptibility mapping. **Revista Brasileira de Geomorfologia**, v. 18, n. 4, p. 719-735, 2017. DOI: 10.20502/rgb.v18i4.1117
11. DUTILLEUL, J.; BOURLANGE, S.; CONIN, M.; GÉRAUD, Y. Quantification of bound water content, interstitial porosity and fracture porosity in the sediments entering the North Sumatra subduction zone from Cation Exchange Capacity and IODP Expedition 362 resistivity data. **Marine and Petroleum Geology**, v. 111, p. 156–165, 2020. DOI: 10.1016/j.marpetgeo.2019.08.007
12. ENANG, R. K.; KIPS, P. A.; YERIMA, B. P. K.; KOME, G. K.; VAN RANST, E. Pedotransfer functions for cation exchange capacity estimation in highly weathered soils of the tropical highlands of NW Cameroon. **Geoderma Regional**, v. 29, p. e00514, 2022. DOI: 10.1016/j.geodrs.2022.e00514
13. FIANTIS, D.; NELSON, M.; SHAMSHUDDIN, J.; GOH, T. B.; VAN RANST, E. Changes in the chemical and mineralogical properties of Mt. Talang volcanic ash in West Sumatra during the initialweathering phase. **Communications in Soil Science and Plant Analysis**, v. 42, n. 5, p. 569–585, 2011. DOI: 10.1080/00103624.2011.546928
14. FIANTIS, D.; NELSON, M.; SHAMSHUDDIN, J.; GOH, T. B.; VAN RANST, E. Determination of the Geochemical Weathering Indices and Trace Elements Content of New Volcanic Ash Deposits from Mt. Talang (West Sumatra) Indonesia. **Eurasian Soil Science**, v. 43, n. 13, p. 1477–1485, 2010. DOI: 10.1134/S1064229310130077
15. FIANTIS, D.; NELSON, M.; VAN RANST, E.; SHAMSHUDDIN, J.; QAFOKU, N. P. Chemical weathering of new pyroclastic deposits from Mt. Merapi (Java), Indonesia. **Journal of Mountain Science**, v. 6, n. 3, p. 240–254, 2009. DOI: 10.1007/s11629-009-1041-3
16. GIAMBASTIANI, Y.; ERRICO, A.; PRETI, F.; GUASTINI, E.; CENSINI, G. Indirect root distribution characterization using electrical resistivity tomography in different soil conditions. **Urban Forestry and Urban Greening**, v. 67, p. 127442, 2022. DOI: 10.1016/j.ufug.2021.127442
17. HASAN, M.; SHANG, Y.; JIN, W.; AKHTER, G. Estimation of hydraulic parameters in a hard rock aquifer using integrated surface geoelectrical method and pumping test data in southeast Guangdong, China. **Geosciences Journal**, v. 25, n. 2, p. 223–242, 2021. DOI: 10.1007/s12303-020-0018-7
18. HIGHLAND, L. M.; BOBROWSKY, P. The landslide Handbook - A guide to understanding landslides. **US Geological Survey Circular**, v. 1325, p. 1–147, 2008. DOI: 10.3133/cir1325
19. HUNGR, O.; LEROUEIL, S.; PICARELLI, L. The Varnes classification of landslide types, an update. **Landslides**, v. 11, n. 2, p. 167–194, 2014. DOI: 10.1007/s10346-013-0436-y
20. ISMAIL, N.; YANIS, M.; ASYQARI, A. The use of magnetic and geoelectrical methods to locate buried ancient artificial canals and wells around the cultural heritage of Indrapatra Fort, Aceh, Indonesia. **Geosciences Journal**, v. 27, n. 1, p. 67–76, 2022. DOI: 10.1007/s12303-022-0025-y
21. JOSHI, M.; PRASOBH, P. R.; RAJAPPAN, S.; RAO, B. P.; GOND, A.; MISRA, A.; ELDHOSE, K.; NANDAKUMAR, V.; TOMSON, J. K. Detection of soil pipes through remote sensing and electrical resistivity method: Insight from southern Western Ghats, India. **Quaternary International**, v. 575–576, p. 51–61, 2021. DOI: 10.1016/j.quaint.2020.08.021
22. JUHADI; PRATIWI, E. S.; TRIHATMOKO, E.; FINDAYANI, A.; SARTOHADI, J.; HAMID, N. The study of anthropogenic disturbance on geopedogenetic process at the lower slope of Mt. Ungaran, Indonesia. **Revista Brasileira de Geomorfologia**, v. 23, n. 3, p. 1735-1752, 2022. DOI: 10.20502/rbg.v23i3.2142
23. LEE, E. M.; JONES, D. K. C. **Landslide Risk Assessment**. London: Thomas Telford Publishing, 2004. 454p.
24. LOWE, M. A.; MCGRATH, G.; MATHES, F.; LEOPOLD, M. Evaluation of surfactant effectiveness on water repellent soils using electrical resistivity tomography. **Agricultural Water Management**, v. 181, p. 56–65, 2017. DOI: 10.1016/j.agwat.2016.11.013
25. MALICK ROSVELT, D. M.; JEAN VICTOR, K.; ISAAC YANNICK, B.; FRANÇOIS, N.; ARMAND SYLVAIN LUDOVIC, W. Geotechnical soil mapping from electrical and mechanical properties: Case study of the Bafoussam urban area, west

Cameroon. **Applied Computing and Geosciences**, v. 13, p. 100078, 2022. DOI: 10.1016/j.acags.2021.100078

26. MELO, L. B. B. DE; SILVA, B. M.; PEIXOTO, D. S.; CHIARINI, T. P. A.; DE OLIVEIRA, G. C.; CURI, N. Effect of compaction on the relationship between electrical resistivity and soil water content in Oxisol. **Soil and Tillage Research**, v. 208, 2021. DOI: 10.1016/j.still.2020.104876
27. MERRITT, A. J.; CHAMBERS, J. E.; WILKINSON, P. B.; WEST, L. J.; MURPHY, W.; GUNN, D.; UHLEMANN, S. Measurement and modelling of moisture-electrical resistivity relationship of fine-grained unsaturated soils and electrical anisotropy. **Journal of Applied Geophysics**, v. 124, p. 155–165, 2016. DOI: 10.1016/j.jappgeo.2015.11.005
28. MIRACAPILLO, C.; MOREL-SEYTOUX, H. Preliminary Field Tests to Determine the Soil Water Content Using Resistivity Measurements. **Procedia Environmental Sciences**, v. 25, p. 158–165, 2015. DOI: 10.1016/j.proenv.2015.04.022
29. NOVIYANTO, A.; SARTOHADI, J.; PURWANTO, B. H. The distribution of soil morphological characteristics for landslide-impacted Sumbing Volcano, Central Java - Indonesia. **Geoenvironmental Disasters**, v. 7, n. 1, 2020. DOI: 10.1186/s40677-020-00158-8
30. PRATIWI, E. S.; SARTOHADI, J.; WAHYUDI. Geoelectrical Prediction for Sliding Plane Layers of Rotational Landslide at the Volcanic Transitional Landscapes in Indonesia. **IOP Conference Series: Earth and Environmental Science**, v. 286, n. 1, 2019. DOI: 10.1088/1755-1315/286/1/012028
31. PULUNGAN, N. A.; SARTOHADI, J. Variability of Soil Development in Hilly Region, Bogowonto Catchment, Java, Indonesia. **International Journal of Soil Science**, v. 13, n. 1, p. 1–8, 2017. DOI: 10.3923/ijss.2018.1.8
32. PULUNGAN, N. A.; SARTOHADI, J. New Approach to Soil Formation in the Transitional Landscape Zone: Weathering and Alteration of Parent Rocks. **Journal of Environments**, v. 5, n. 1, p. 1–7, 2018. DOI: 10.20448/journal.505.2018.51.1.7
33. REKAPALLI, R., P, P. D.; SARMA, V. S.; PRASAD, P. R. Electrical resistivity imaging over natural (in situ) geological samples using physical model studies. **Arabian Journal of Geosciences**, v. 7, n. 11, p. 4717–4725, 2014. DOI: 10.1007/s12517-013-1101-4
34. REVIL, A.; COPEREY, A.; SHAO, Z.; FLORSCH, N.; FABRICIUS, I. L.; DENG, Y.; DELSMAN, J. R.; PAUW, P. S.; KARAOULIS, M.; DE LOUW, P. G. B.; VAN BAAREN, E. S.; DABEKAUSSEN, W.; MENKOVIC, A.; GUNNINK, J. L. Complex conductivity of soils. **Water Resources Research**, v. 53, n. 8, p. 7121–7147, 2017. DOI: 10.1002/2017WR020655
35. SAMOUËLIAN, A.; COUSIN, I.; TABBAGH, A.; BRUAND, A.; RICHARD, G. Electrical resistivity survey in soil science: A review. **Soil and Tillage Research**, v. 83, n. 2, p. 173–193, 2005. DOI: 10.1016/j.still.2004.10.004
36. SARTOHADI, J.; HARLIN JENNIE PULUNGAN, N. A.; NURUDIN, M.; WAHYUDI, W. The ecological perspective of landslides at soils with high clay content in the middle bogowonto watershed, central Java, Indonesia. **Applied and Environmental Soil Science**, v. 2018, 2018. DOI: 10.1155/2018/2648185
37. SCHWARTZ, B. F.; SCHREIBER, M. E.; YAN, T. Quantifying field-scale soil moisture using electrical resistivity imaging. **Journal of Hydrology**, v. 362, n. 3–4, p. 234–246, 2008. DOI: 10.1016/j.jhydrol.2008.08.027
38. SÉGER, M.; COUSIN, I.; FRISON, A.; BOIZARD, H.; RICHARD, G. Characterisation of the structural heterogeneity of the soil tilled layer by using in situ 2D and 3D electrical resistivity measurements. **Soil and Tillage Research**, v. 103, n. 2, p. 387–398, 2009. DOI: 10.1016/j.still.2008.12.003
39. SINGH, S.P.; PRADHAN, V.; VISHAL, T. N. **Landslides: Theory, Practice and Modelling (Vol. 50)**. New York City: Springer International Publishing, 2019. 313p.
40. SINGLA, R.; ALEX, T. C.; KUMAR, R. On mechanical activation of glauconite: Physicochemical changes, alterations in cation exchange capacity and mechanisms. **Powder Technology**, v. 360, p. 337–351, 2020. DOI: 10.1016/j.powtec.2019.10.035
41. SONG, X.; CHEN, C.; ARTHUR, E.; TULLER, M.; ZHOU, H.; SHANG, J.; REN, T. Cation exchange capacity and soil pore system play key roles in water vapour sorption. **Geoderma**, v. 424, p. 116017, 2022. DOI: 10.1016/j.geoderma.2022.116017
42. SUN, H.; WANG, Y.; ZHAO, Y.; ZHANG, P.; SONG, Y.; HE, M.; ZHANG, C.; TONG, Y.; ZHOU, J.; QI, L.; XU, L. Assessing

the value of electrical resistivity derived soil water content: Insights from a case study in the Critical Zone of the Chinese Loess Plateau. **Journal of Hydrology**, v. 589, p. 125132, 2020. DOI: 10.1016/j.jhydrol.2020.125132

43. TELFORD, W. M.; GELDART, L. P.; SHERIFF, R. E.; KEYS, D. A. **Applied Geophysics**. New York: Press Syndicate of the Cambridge University Press, 1990. 744p.
44. WEISENBERGER, T. B.; INGIMARSSON, H.; HERSIR, G. P.; FLÓVENZ, Ó. G. Cation-exchange capacity distribution within hydrothermal systems and its relation to the alteration mineralogy and electrical resistivity. **Energies**, v. 13, n. 21, p. 1–19, 2020. DOI: 10.3390/en13215730
45. WIDA, W. A.; MAAS, A.; SARTOHADI, J. Pedogenesis of Mt. Sumbing Volcanic Ash above The Alteration Clay Layer in The Formation of Landslide Susceptible Soils in Bompon Sub-Watershed. **Ilmu Pertanian (Agricultural Science)**, v. *4*, n. 1, p. 15, 2019. DOI: 10.22146/ipas.41893
46. ZHAO, D.; LI, N.; ZARE, E.; WANG, J.; TRIANTAFILIS, J. Mapping cation exchange capacity using a quasi-3d joint inversion of EM38 and EM31 data. **Soil and Tillage Research**, v. 200, 2020. DOI: 10.1016/j.still.2020.104618
47. ZUO, F. L.; LI, X. Y.; YANG, X. F.; MA, Y. J.; SHI, F. Z.; LIAO, Q. W.; LI, D. S.; WANG, Y.; WANG, R. D. Linking root traits and soil moisture redistribution under Achnatherum splendens using electrical resistivity tomography and dye experiments. **Geoderma**, v. 386, p. 114908, 2021. DOI: 10.1016/j.geoderma.2020.114908